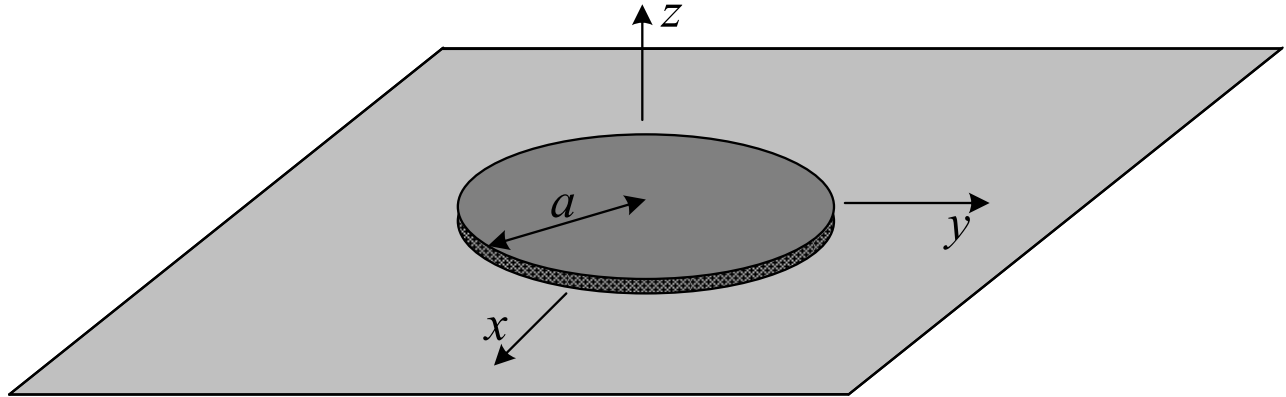


LECTURE 22: MICROSTRIP ANTENNAS – PART III

(Circular patch antennas: the cavity model. Radiation field of the circular patch. Circularly polarized radiation from patches. Arrays and feed networks.)

1. Circular patch: the cavity model



The circular patch cannot be analyzed using the TL method, but can be accurately described by the cavity method. It is again assumed that only TM_z modes are supported in the cavity. They are fully described by the VP $\mathbf{A} = A_z \hat{\mathbf{z}}$. The A_z VP function satisfies the Helmholtz equation,

$$\nabla^2 A_z + k^2 A_z = 0 \quad (22.1)$$

which now is solved in cylindrical coordinates:

$$\frac{1}{\rho} \frac{\partial}{\partial \rho} \left(\rho \frac{\partial A_z}{\partial \rho} \right) + \frac{1}{\rho^2} \frac{\partial^2 A_z}{\partial \phi^2} + \frac{\partial^2 A_z}{\partial z^2} + k^2 A_z = 0, \quad (22.2)$$

$$\Rightarrow \frac{1}{\rho} \frac{\partial A_z}{\partial \rho} + \frac{\partial^2 A_z}{\partial \rho^2} + \frac{1}{\rho^2} \frac{\partial^2 A_z}{\partial \phi^2} + \frac{\partial^2 A_z}{\partial z^2} + k^2 A_z = 0, \quad (22.3)$$

Using the method of separation of variables,

$$A_z = R(\rho)F(\phi)Z(z), \quad (22.4)$$

$$\Rightarrow \frac{1}{\rho} FZ \frac{\partial R}{\partial \rho} + FZ \frac{\partial^2 R}{\partial \rho^2} + \frac{RZ}{\rho^2} \frac{\partial^2 F}{\partial \phi^2} + RF \frac{\partial^2 Z}{\partial z^2} + k^2 RFZ = 0, \quad (22.5)$$

$$\Rightarrow \frac{1}{\rho R} \frac{\partial R}{\partial \rho} + \frac{1}{R} \frac{\partial^2 R}{\partial \rho^2} + \frac{1}{\rho^2 F} \frac{\partial^2 F}{\partial \phi^2} + \frac{1}{Z} \frac{\partial^2 Z}{\partial z^2} = -k^2. \quad (22.6)$$

The 4th term is independent of ρ and ϕ , and is being separated:

$$\frac{1}{Z} \frac{\partial^2 Z}{\partial z^2} = -k_z^2. \quad (22.7)$$

Then,

$$\frac{1}{R\rho} \frac{\partial R}{\partial \rho} + \frac{1}{R} \frac{\partial^2 R}{\partial \rho^2} + \frac{1}{\rho^2 F} \frac{\partial^2 F}{\partial \phi^2} = -(k^2 - k_z^2) = \text{const.} \quad (22.8)$$

$$\Rightarrow \frac{\rho}{R} \frac{\partial R}{\partial \rho} + \frac{\rho^2}{R} \frac{\partial^2 R}{\partial \rho^2} + \frac{1}{F} \frac{\partial^2 F}{\partial \phi^2} + (k^2 - k_z^2) \rho^2 = 0. \quad (22.9)$$

Now, the 3rd term is independent of ρ , and the other terms are independent of ϕ . Thus, (22.9) is separated into two equations:

$$\frac{1}{F} \frac{\partial^2 F}{\partial \phi^2} = k_\phi^2 \quad (22.10)$$

and

$$\frac{\rho}{R} \frac{\partial R}{\partial \rho} + \frac{\rho^2}{R} \frac{\partial^2 R}{\partial \rho^2} + (k^2 - k_z^2) \rho^2 - k_\phi^2 = 0. \quad (22.11)$$

We define

$$k_\rho^2 = k^2 - k_z^2. \quad (22.12)$$

Then (22.11) can be written as [note that (22.11) depends only on ρ]:

$$\rho \frac{\partial}{\partial \rho} \left(\rho \frac{\partial R}{\partial \rho} \right) + [(k_\rho \rho)^2 - k_\phi^2] \cdot R = 0. \quad (22.13)$$

Thus, equation (22.1) has been separated into three ordinary differential equations — (22.7), (22.10) and (22.13).

A. The Z-equation

Equation (22.7) is complemented by the Neumann BC at the top patch and the grounded plane (electric walls):

$$\frac{\partial A_z}{\partial z} = 0 \Rightarrow \frac{\partial Z}{\partial z} = 0. \quad (22.14)$$

Its solution, therefore, is in the form

$$\boxed{Z(z) = \sum_p c_p \cos\left(p \frac{\pi}{h} z\right)} \quad (22.15)$$

with the eigenvalues are $k_z = p\pi / h$. Here, p is an integer.

B. The F -equation

The solution of (22.10) is also a harmonic function. We are interested in real-valued harmonic functions, i.e.,

$$F(\phi) = \sum_n b_n^c \cos(k_\phi^n \phi) + b_n^s \sin(k_\phi^n \phi). \quad (22.16)$$

Since there are no specific BC's to be imposed at certain angular positions, the only requirement for the eigenvalues k_ϕ^n comes from the condition that the $F(\phi)$ must be periodic in ϕ ,

$$F(\phi) = F(\phi + 2\pi). \quad (22.17)$$

Equation (22.17) is true only if k_ϕ^n are integers. That is why the usual construction of a general solution for $F(\phi)$ for a complete cylindrical region ($\phi = 0$ to 2π) is in the form

$$F(\phi) = \sum_n b_n^c \cos(n\phi) + b_n^s \sin(n\phi) \quad (22.18)$$

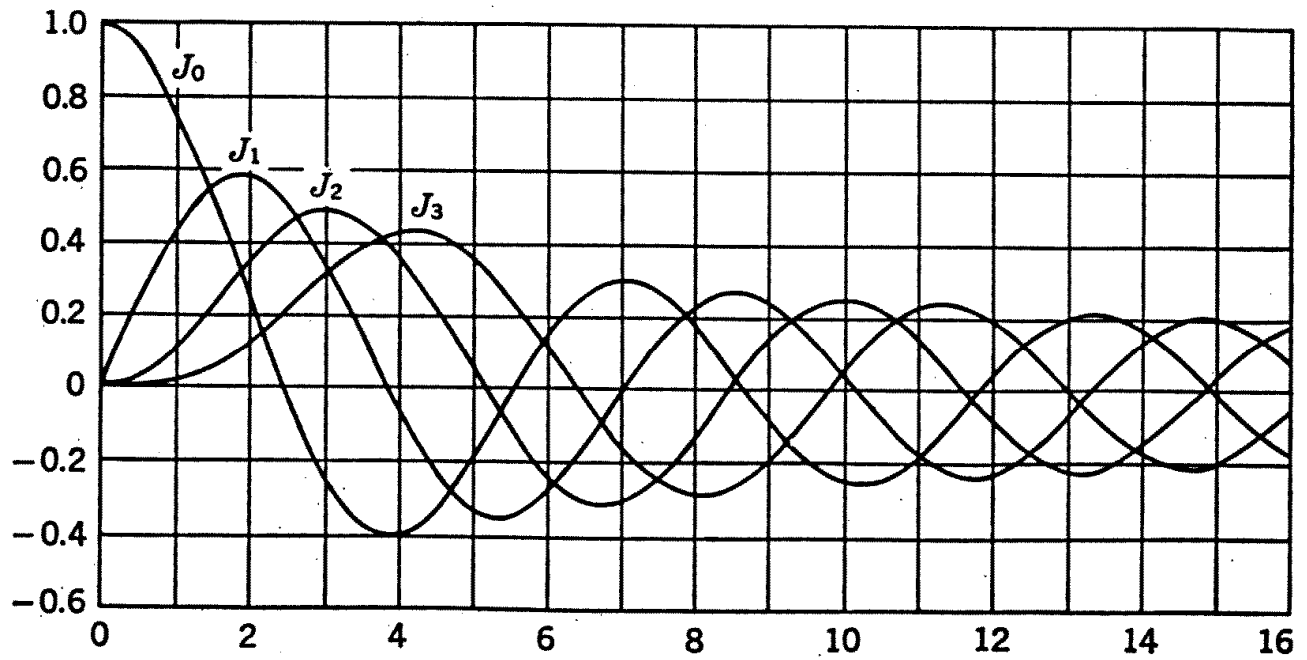
where n is an integer. This is the well-known Fourier-series expansion.

C. The R -equation

Equation (22.13) is a Bessel equation in which k_ϕ is an integer ($k_\phi = n$). Solutions are of the form of the following special functions:

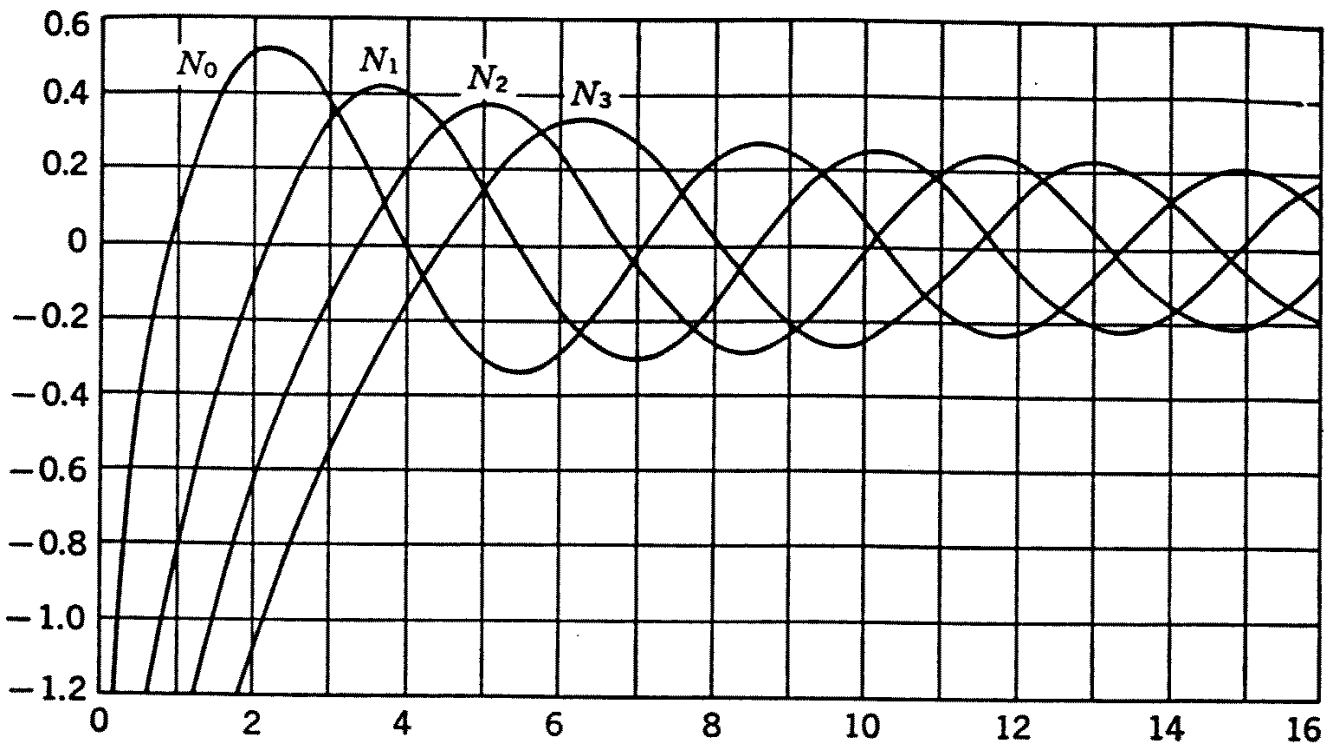
- $J_n(k_\rho \rho)$ — Bessel function of the first kind,
- $N_n(k_\rho \rho)$ — Bessel function of the second kind (Neumann function),
- $H_n^{(1)}(k_\rho \rho)$ — Hankel function of the first kind,
- $H_n^{(2)}(k_\rho \rho)$ — Hankel function of the second kind.

Note: $H_n^{(1)} = J_n + jN_n$; $H_n^{(2)} = J_n - jN_n$.



Bessel functions of the first kind.

Fig. D-1, Harrington, p. 461



Bessel functions of the second kind.

Fig. D-2, Harrington, p. 462

The eigenvalues are determined according to the boundary conditions. In the cavity model, it is required that (magnetic wall)

$$\frac{\partial A_z}{\partial \rho} = 0 \Rightarrow \frac{\partial R}{\partial \rho} = 0 \Big|_{\rho=a}, \quad (22.19)$$

and that the field is finite for $\rho = a$. The Bessel functions of the first kind $J_n(k_\rho \rho)$ are the suitable choice. The eigenvalues k_ρ are determined from (22.19):

$$\frac{\partial J_n(k_\rho \rho)}{\partial \rho} = 0 \Big|_{\rho=a}, \Rightarrow k_\rho^{nm} = \frac{\chi'_{nm}}{a}, \quad (22.20)$$

where χ'_{nm} is the m^{th} null of the derivative of the Bessel function of the n^{th} order J'_n . Thus, the solution of the Helmholtz equation for A_z can be given in a modal form as, see (22.4),

$$A_z^{(mnp)} = M_{mnp} J_m \left(\chi'_{nm} \frac{\rho}{a} \right) \cdot [b_n^c \cos(n\phi) + b_n^s \sin(n\phi)] \cdot \cos \left(p \frac{\pi}{h} z \right). \quad (22.21)$$

The characteristic equation (22.12) is finally obtained as

$$k^2 = \omega^2 \mu \varepsilon = k_\rho^2 + k_z^2. \quad (22.22)$$

From (22.22), the resonant frequencies of the patch can be obtained:

$$\mu \varepsilon \omega_{mnp}^2 = \left(\frac{\chi'_{nm}}{a} \right)^2 + \left(p \frac{\pi}{h} \right)^2, \quad (22.23)$$

$$f_{r(mnp)} = \frac{1}{2\pi \sqrt{\mu \varepsilon}} \sqrt{\left(\frac{\chi'_{nm}}{a} \right)^2 + \left(p \frac{\pi}{h} \right)^2}. \quad (22.24)$$

Equation (22.24) does not take into account the fringing effect of the circular patch. To account for the effective increase of the patch size due to fringing, the actual radius a is replaced by an effective one,

$$a_e = a \left\{ 1 + \frac{2h}{\pi a \varepsilon_r} \left[\ln \left(\frac{\pi a}{2h} \right) + 1.7726 \right] \right\}^{1/2}. \quad (22.25)$$

The first four modes in ascending order are TM_{z110} , TM_{z210} , TM_{z010} ,

TM_{z310} where the respective nulls χ'_{nm} are

$$\begin{aligned}\chi'_{11} &= 1.8412 & \chi'_{01} &= 3.8318 \\ \chi'_{21} &= 3.0542 & \chi'_{31} &= 4.2012\end{aligned}$$

The resonant frequency of the dominant TM_{z110} mode can be determined from (22.25) as

$$f_{r(110)} = \frac{1.8412 \cdot c}{2\pi a_e \sqrt{\epsilon_r}} \quad (22.26)$$

where c is the speed of light in vacuum.

The VP of the dominant TM_{z110} mode is

$$A_z^{(110)} = M_{110} J_1 \left(\chi'_{11} \frac{\rho}{a} \right) \cdot (b_n^c \cos \phi + b_n^s \sin \phi). \quad (22.27)$$

Assuming excitation at $\phi = 0$ (A_z has vanishing angular first derivative), we set $b_n^s = 0$. The field components are computed from A_z according to the field-potential relations

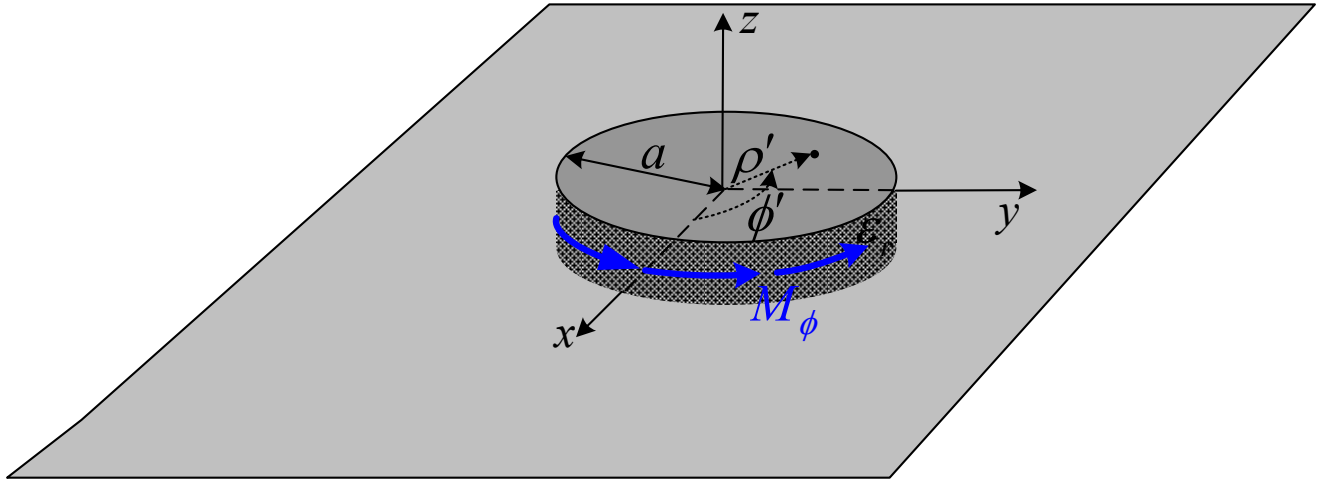
$$\begin{aligned}E_\rho &= -\frac{j}{\omega\mu\epsilon} \frac{\partial^2 A_z}{\partial\rho\partial z} & H_\rho &= \frac{1}{\mu} \frac{1}{\rho} \frac{\partial A_z}{\partial\phi} \\ E_\phi &= -\frac{j}{\omega\mu\epsilon} \frac{1}{\rho} \frac{\partial^2 A_z}{\partial\phi\partial z} & H_\phi &= -\frac{1}{\mu} \frac{\partial A_z}{\partial\rho} \\ E_z &= -\frac{j}{\omega\mu\epsilon} \left(\frac{\partial^2 A_z}{\partial z^2} + k^2 A_z \right) & H_z &= 0\end{aligned} \quad (22.28)$$

For the dominant TM_{z110} mode,

$$\begin{aligned}E_\rho = E_\phi &= 0 & H_\rho &= j \frac{E_0}{\omega\mu_0} \frac{1}{\rho} J_1(\chi'_{11}\rho/a) \sin\phi \\ E_z &= E_0 J_1(\chi'_{11}\rho/a) \cos\phi & H_\phi &= j \frac{E_0}{\omega\mu_0} J'_1(\chi'_{11}\rho/a) \cos\phi\end{aligned} \quad (22.29)$$

From the field components, we can compute the cavity modal impedance for any feed point specified by ρ and ϕ . In view of the closed-wall nature of the BCs, the impedance will be reactive. To obtain the real part of the antenna impedance, the radiated power has to be computed.

2. Radiated fields and equivalent surface currents of the circular patch



As with the rectangular patch, the field radiated by the circular slot is determined using the equivalence principle. The circumferential wall of the cavity is replaced by an equivalent circular sheet of magnetic current density

$$M_{s\phi} = 2E_z|_{\rho=a}, \text{ V/m}, \quad (22.30)$$

radiating in free space. The factor of 2 accounts for the ground plane. Since the height of the slot h is very small and the slot field is independent of z , we can substitute the surface magnetic current density over the slot with a filamentary magnetic current $I_m = M_{s\phi}h$:

$$I_m = \underbrace{2hE_0J_1(\chi'_{11})}_{2V_0} \cos \phi, \text{ V}. \quad (22.31)$$

Here, $V_0 = hE_0J_1(\chi'_{11})$ is the voltage between ground and the top plate of the patch at the feed ($\phi = 0$).

Using the theory for the radiation field of a circular slot, the following expressions are obtained for the far field of the circular patch:

$$E_r = 0, E_\theta = -C(r) \cdot \cos \phi \cdot J'_{02}, E_\phi = C(r) \cdot \cos \theta \sin \phi \cdot J_{02}, \quad (22.32)$$

where

$$C(r) = j \frac{k_0 a_e V_0 e^{-jk_0 r}}{2r},$$

$$J_{02} = J_0(k_0 a_e \sin \theta) + J_2(k_0 a_e \sin \theta),$$

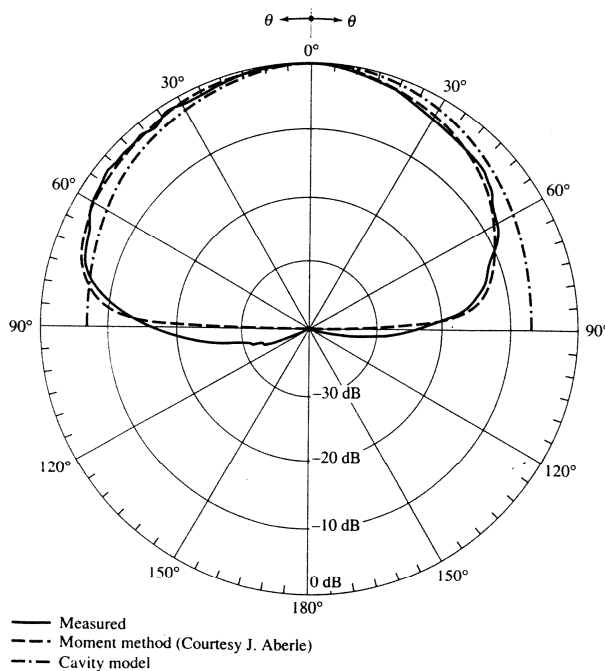
$$J'_{02} = J_0(k_0 a_e \sin \theta) - J_2(k_0 a_e \sin \theta).$$

E-plane amplitude pattern:

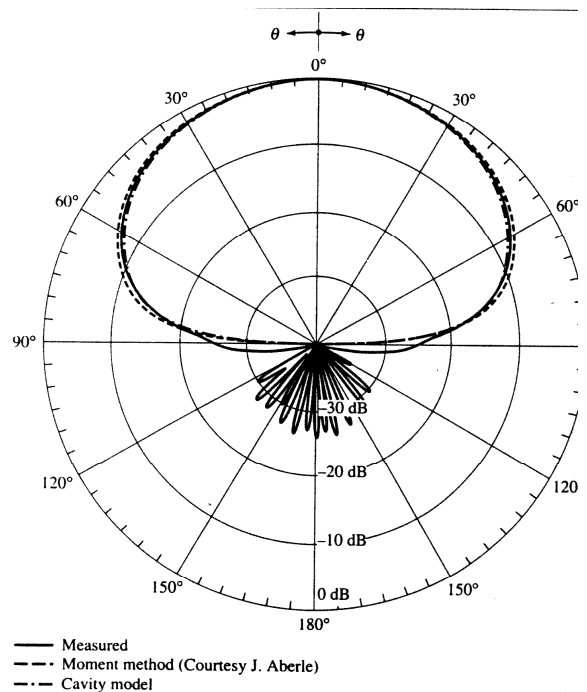
$$\bar{E}_\theta(0^\circ \leq \theta \leq 90^\circ, \varphi = 0^\circ, 180^\circ) = J'_{02}, \quad \bar{E}_\phi = 0$$

H-plane amplitude pattern:

$$\bar{E}_\phi(0^\circ \leq \theta \leq 90^\circ, \varphi = 90^\circ, 270^\circ) = \cos \theta \cdot J_{02}, \quad \bar{E}_\theta = 0$$



(a) E-plane ($\phi = 0^\circ, 180^\circ$)



(a) H-plane ($\phi = 90^\circ, 270^\circ$)

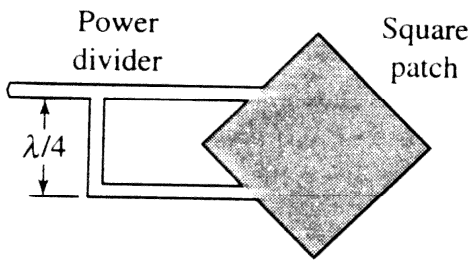
Measured and computed (based on moment method and cavity models) E- and H-plane patterns of circular microstrip patch antenna ($a = 0.525$ cm, $a_e = 0.598$ cm, $\gamma_f = 0.1$ cm, $\epsilon_r = 2.2$, $h = 0.1588$ cm, $f_0 = 10$ GHz, $\lambda_0 = 3$ cm).

Fig. 14.23, p. 758, Balanis

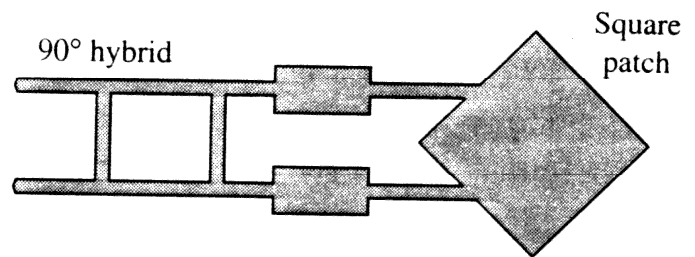
3. Circular polarization with patch antennas

Circular polarization can be obtained if two orthogonal modes are excited with a 90° time-phase difference between them. This can be accomplished by adjusting the physical dimensions of the patch and using either one or two feed points.

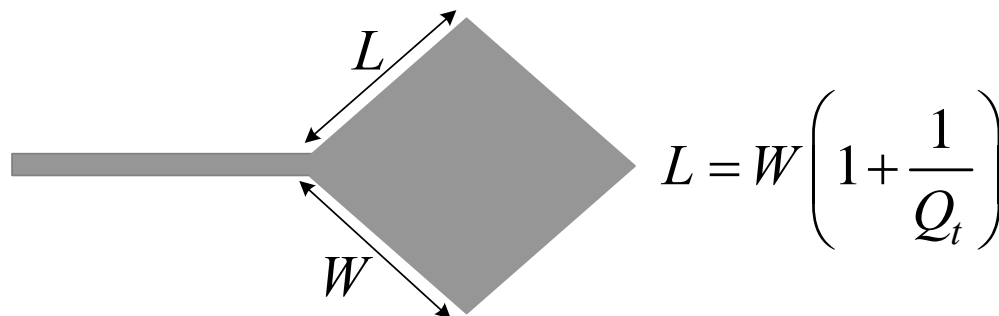
A. Square patch with circularly polarized field



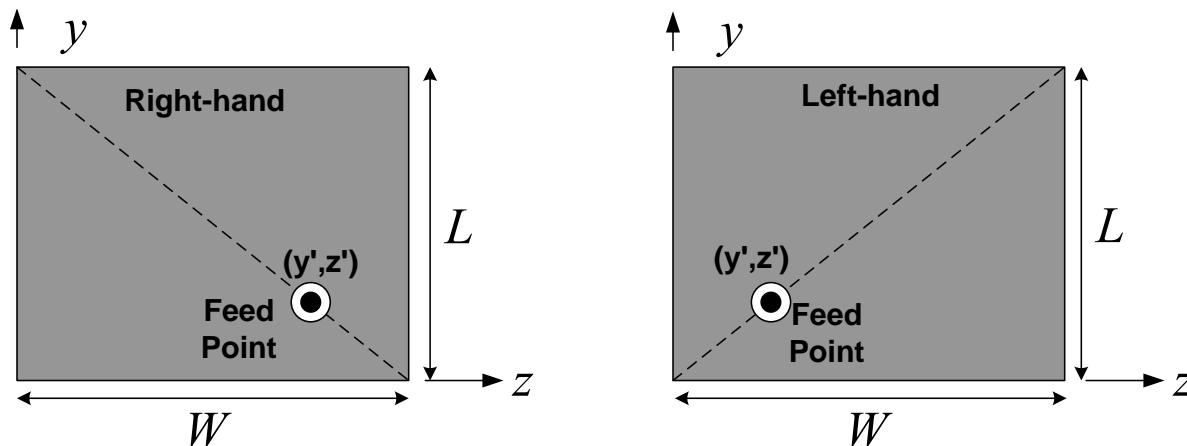
(a) Square patch driven at adjacent sides through a power divider



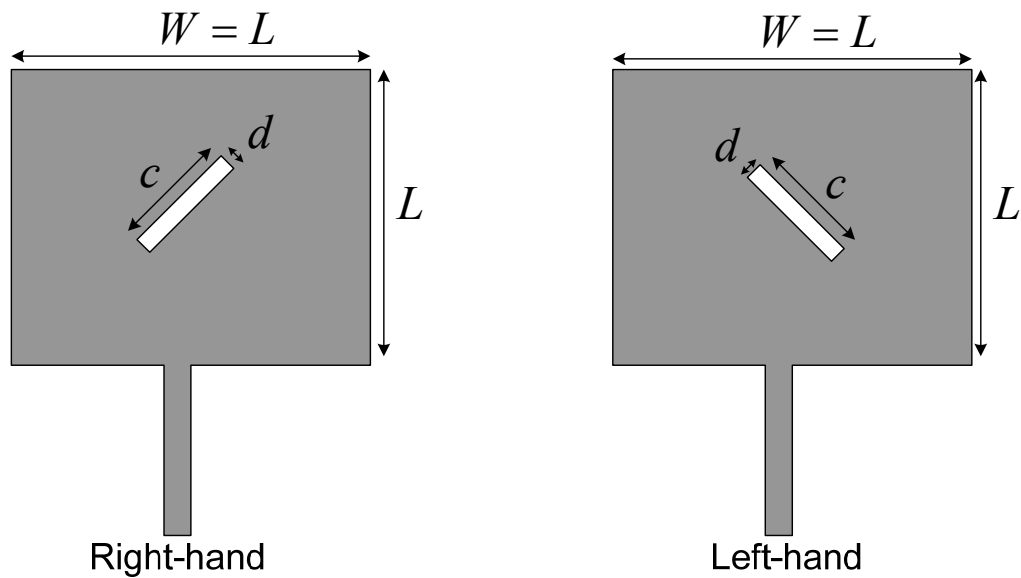
(b) Square patch driven at adjacent sides through a 90° hybrid



(c) Nearly square patch with microstrip-line feed for CP accounting for losses; $Q_t = 1 / \tan \delta_{eff}$

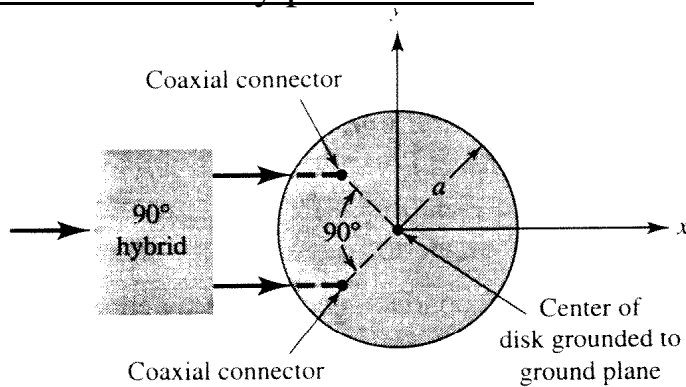


(d) Coax-feeds for CP

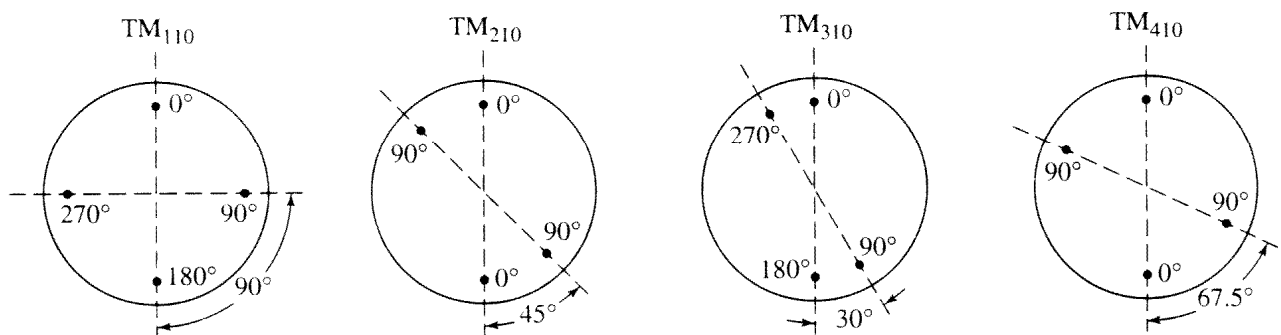


(e) CP for square patches with thin slots: $c = L / 2.72 = W / 2.72$, $d = c / 10$

B. Circular patch with circularly polarized field



(c) Circular patch fed with coax



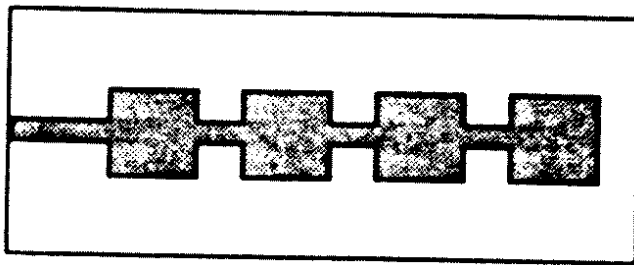
(d) Circular patch feed arrangements for TM_{110}^z and higher order modes

(Source: J. Huang, "Circularly Polarized Conical Patterns from Circular Microstrip Antennas," IEEE Trans. Antennas Propagat., Vol. AP-32, No. 9, Sept. 1984. © 1984 IEEE.)

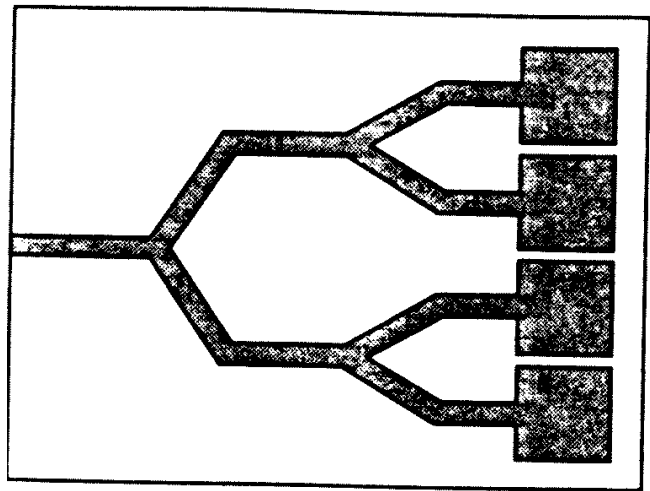
FEED-PROBE ANGULAR SPACING OF DIFFERENT MODES FOR CIRCULAR POLARIZATION

	TM_{110}	TM_{210}	TM_{310}	TM_{410}	TM_{510}	TM_{610}
α	90°	45° or 135°	30° or 90°	22.5° or 67.5°	$18^\circ, 54^\circ$ or 90°	$15^\circ, 45^\circ$ or 75°

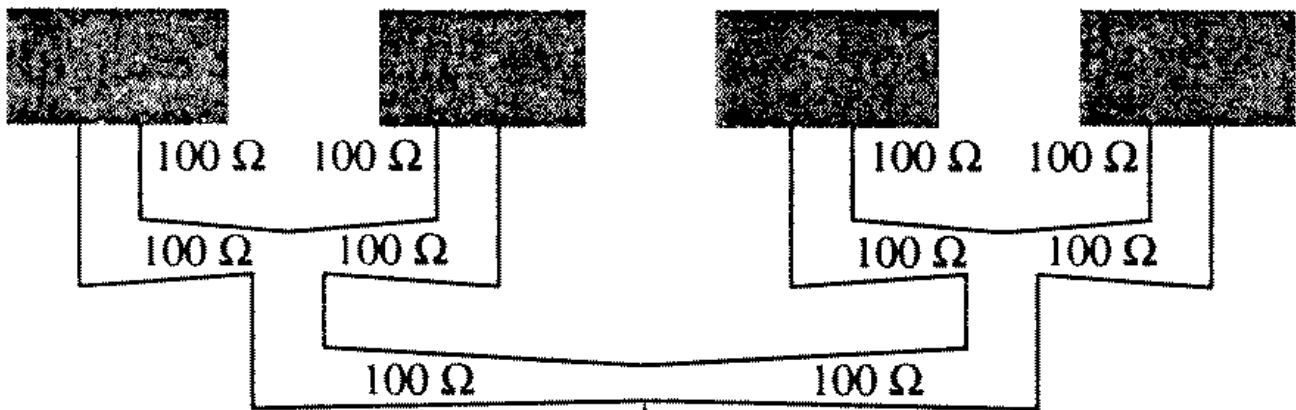
4. Array and feed networks



(a) Series feed

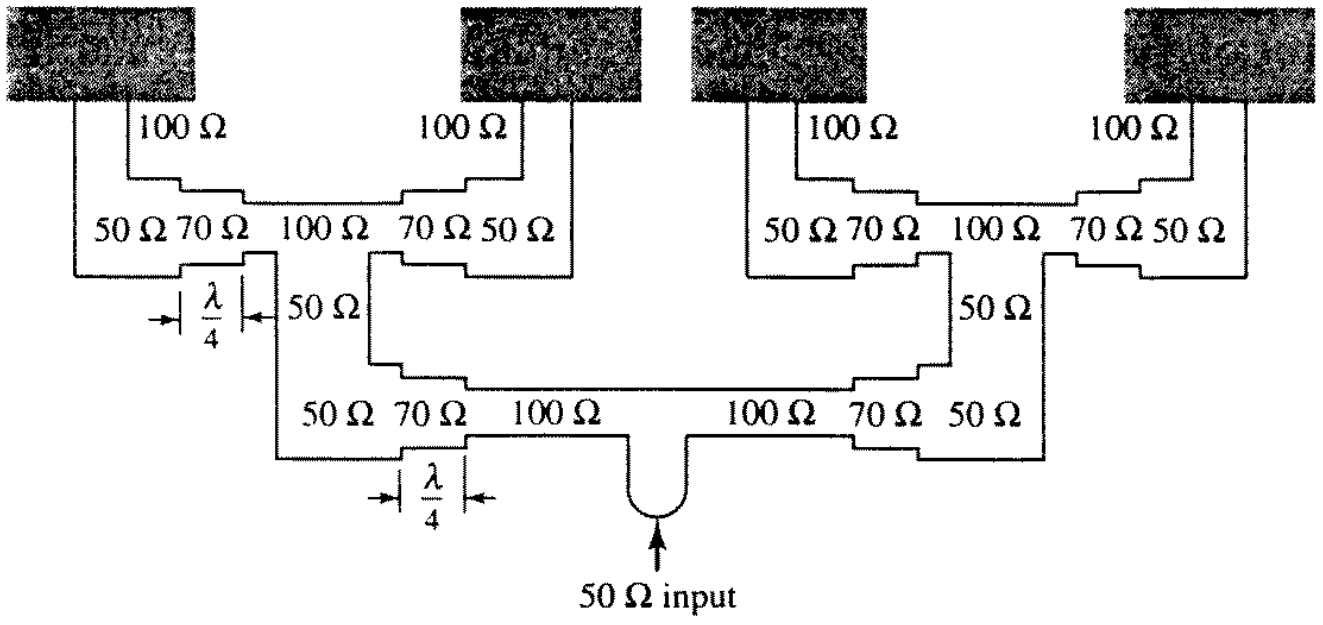


(b) Corporate feed



50 Ω input

(a) Tapered lines



(b) $\lambda/4$ transformers